Eurasian Chem.-Technol. J. 27 (2025) 127–138
The journal of the Institute of Combustion Problems https://ect-journal.kz

https://doi.org/10.18321/ectj1660

Combined Computational and Experimental Study of Inclusion Complexes of Lupinine and its 1,2,3-triazole Derivative with β-cyclodextrin

Zh.S. Nurmaganbetov[1,2], S.D. Fazylov[1]*, O.A. Nurkenov[1], A.Zh. Sarsenbekova[3], I.A. Pustolaikina[3], O.T. Seilkhanov[4], A.K. Sviderskiy[5], Ye.V. Minayeva[3]

[1]Institute of Organic Synthesis and Coal Chemistry of the Republic of Kazakhstan, Alikhanov str., 1, Karaganda, Kazakhstan
[2]Karaganda Medical University, Gogol str., 40, Karaganda, Kazakhstan
[3]Karaganda Buketov University, Universitetskaya str., 28, Karaganda, Kazakhstan
[4]Kokshetau University of the name of Sh. Ualikhanov, Abay St., 76, Kokshetau, Kazakhstan
[5]Department of Mining, Metallurgy and Natural Sciences, Zhezkazgan University named after O. Baikonurov, Alashakhan ave., 1b, Zhezkazgan, Kazakhstan

Article info

Received:
16 February 2025

Received in revised form:
2 April 2025

Accepted:
25 May 2025

Keywords:
Lupinine alkaloid
β-cyclodextrin
Quinolizidine derivatives
1,2,3-triazoles
Inclusion complexes

Abstract

The study presents the results of obtaining clathrate inclusion complexes of the alkaloid lupinine (**Lup**) and its 1,2,3-triazole derivative (**Lup-T**) using the oligosaccharide β-cyclodextrin (**β-CD**). The structural features of the encapsulated forms of lupinine (Lup) and its derivatives were characterized by molecular modeling, IR spectroscopy, ^{1}H and ^{13}C NMR, as well as two-dimensional ^{1}H-^{1}H (COSY) and ^{1}H-^{13}C (HMBC, HSQC) NMR spectroscopy. A comparative thermal degradation study of lupinine, its triazole derivative, and their inclusion complexes with β-cyclodextrin was performed using differential thermogravimetry (DTG) and differential scanning calorimetry (DSC). The kinetic parameters of the thermal decomposition reactions of lupinine-based substrates at different heating rates, along with the values of apparent activation energy, were calculated using model-free isoconversional methods by Friedman and Ozawa-Flynn-Wall.

1. Introduction

Lupinine (**Lup**) is the simplest representative of a large group of quinolizidine alkaloids found in plants of the genera *Lupinus* and *Anabasis* [1-3]. Pharmacologically, lupinine and its derivatives exhibit bactericidal and sedative effects, possess anti-inflammatory and hypotensive properties, and are of interest as promising pharmacophores [4, 5]. The structural modifiability of the lupinine molecule allows for the targeted synthesis of new compounds and the investigation of their biological properties. Many derivatives of the (−)-lupinine alkaloid have proven to be valuable biologically active compounds [6, 7], which has stimulated their comprehensive study and the development of methods for constructing more complex structures. Among the known lupinine derivatives, esters are the most extensively studied. For example, several lupinine esters have demonstrated strong local anesthetic activity [8-11] and anticholinesterase effects [10-12]. The hydroxyl group in lupinine can be readily converted into an amino group, enabling the synthesis of a wide range of N-substituted derivatives, some of which exhibit anti-inflammatory [13, 14], antihypertensive, antiarrhythmic [15], antimalarial [16-18], and anticholinesterase [19] activities. Additionally, a group of derivatives based on ω-chlorolupinan, ω-thiolupinan, and ω-cyanolupinan has been synthesized as promising ligands for sigma receptors of the central nervous system, which are implicated in the pathogenesis of psychiatric and motor disorders [20].

One of the less explored but promising directions in the structural modification of lupinine is the synthesis of its novel 1,2,3-triazole derivatives. For a long time, triazoles remained a scarcely accessible class of compounds due to the high energetic contri-

*Corresponding author.
E-mail address: iosu8990@mail.ru

bution of a single 1,2,3-triazole ring, which amounts to 168 kJ/mol [21], making their synthesis highly energy-consuming. In recent years, however, this situation has changed significantly due to the introduction of dipolar aprotic solvents and phase-transfer catalysis into the practice of organic synthesis [22-25]. Previously, we reported a series of studies on the synthesis and structural characterization of new (1S,9aR)-((1H-1,2,3-triazol-1-yl)methyl)octahydro-1H-quinolizine derivatives of lupinine [26].

In the present study, we describe the results of investigating the encapsulation of the lupinine (**Lup**) molecule and its 1,2,3-triazole derivative (**Lup-T**) by the starch-derived oligosaccharide β-cyclodextrin (**β-C**D) using molecular modeling, IR spectroscopy, and ^{1}H and ^{13}C NMR spectroscopy. Thermal analysis of lupinine (**Lup**) and its inclusion complex (**Lup-T**) was also carried out using differential thermogravimetry (DTG) and differential scanning calorimetry (DSC). The formation of supramolecular inclusion complexes of lupinine and its novel triazole derivative may serve as a basis for developing a new water-soluble pharmaceutical form.

2. Results and Discussion

2.1 In silico studies

2.1.1 Molecular modeling of the inclusion complexes of lupinine and (1S,9aR)-1-[(4-phenyl-1H-1,2,3-triazol-1-yl) methyl]octahydro-1H-quinolizine with β-cyclodextrin

Initially, molecular modeling and geometry optimization of the studied molecules – lupinine (**Lup**), (1S,9aR)-1-[(4-phenyl-1H-1,2,3-triazol-1-yl)methyl] octahydro-1H-quinolizine (**Lup-T**), and β-cyclodextrin (**β-CD**) – were carried out using the semi-empirical AM1 method implemented in the Gaussian 2016 software package (Figs. 1 and 2).

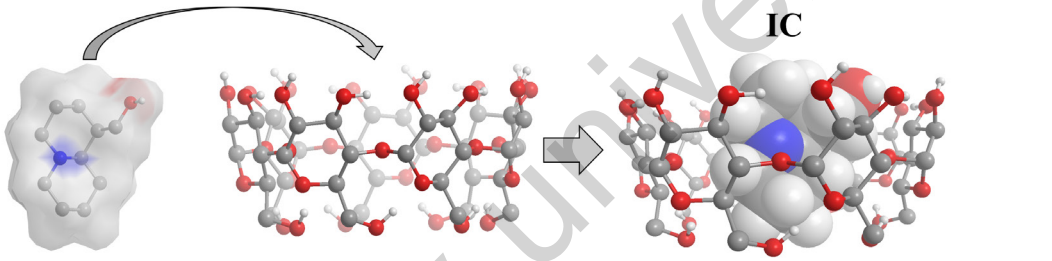

Fig. 1. Structural formulas of Lupinine, β-cyclodextrin and its inclusion complex.

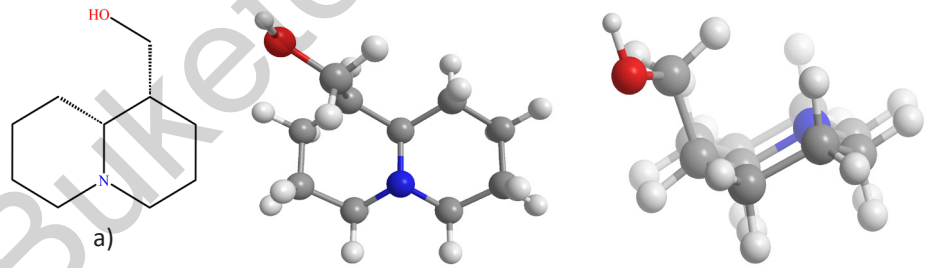

Fig. 2. The lupinine molecule: a) structural formula of lupinine; b), c) 3D model of the lupinine molecule (size ~6 x 7 Å).

The lupinine alkaloid molecule is relatively small in size (~6×7 Å) and contains a quinolizidine heterocycle. The quinolizidine core adopts a trans-configuration, with both rings adopting a chair conformation, and the $–CH_2OH$ group occupying an axial position. The **Lup-T** molecule (Fig. 3) is more voluminous (~6×15 Å); in addition to the quinolizidine heterocycle, its structure includes a side chain composed of sequentially connected triazole and benzene rings. As in the case of lupinine, the quinolizidine core adopts a trans-configuration, both rings adopt chair conformations, and the side chain is oriented axially.

The β-cyclodextrin (**β-CD**) molecule (Fig. 4) is a macrocyclic compound composed of seven glucopyranose units linked by 1,4-glycosidic bonds. The **β-CD** macrocycle has the shape of a hollow truncated cone and features a toroidal internal cavity with an inner diameter of approximately 6.6 Å and a wall height of about 7 Å. The shape of **β-CD** is stabilized by hydrogen bonds between the hydroxyl groups located on the outer surface of the molecule, which also contribute to its good water solubility.

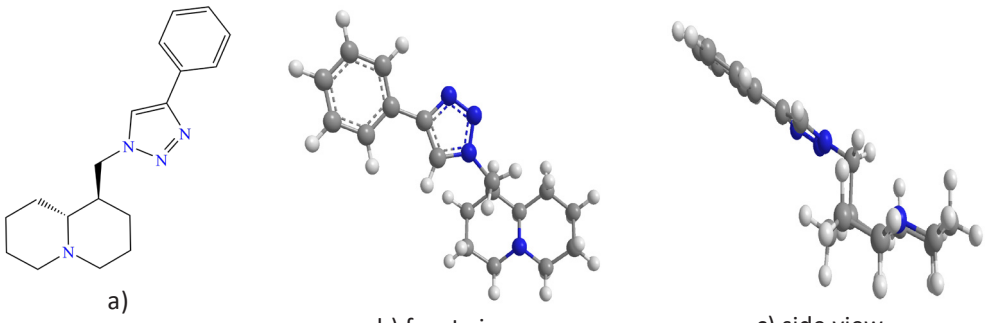

a) b) front view c) side view

Fig. 3. (1S,9aR)-1-[(4-phenyl-1H-1,2,3-triazol-1-yl)methyl]octahydro-1H-quinolizine (**Lup-T**) molecule: a) structural formula of **Lup-T**; b), c) 3D model of the **Lup-T** molecule (size ~6 × 15 Å)

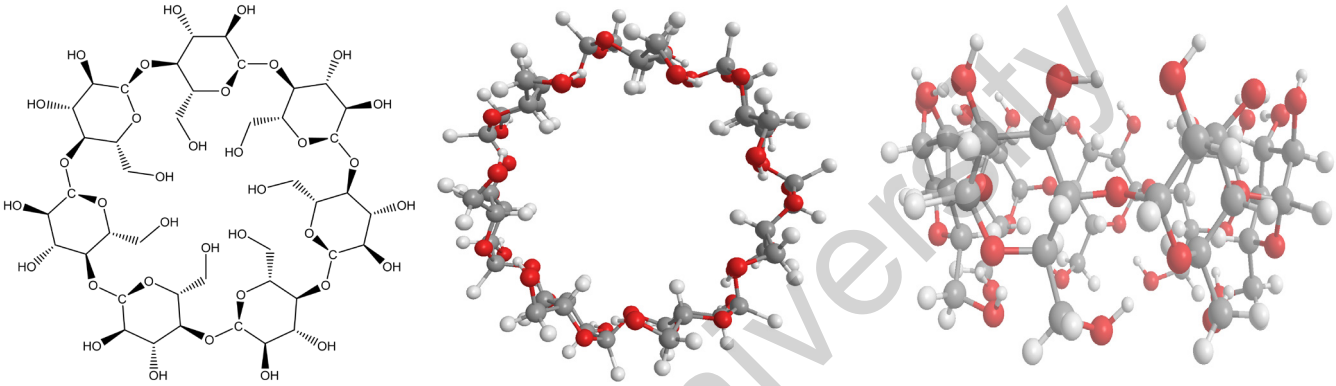

a) b) front view c) side view

Fig. 4. β-CD molecule: a) structural formula; b) ,c) 3D model of the molecule (size ~7 (height) × 13 (diameter) Å).

The obtained computational data indicate that the size of the internal cavity of the β-cyclodextrin molecule is sufficient for the formation of inclusion complexes with lupinine and its derivative, **Lup-T**. As the next step, a study was carried out using the AutoDock 4.2.6 software to determine the binding energy of their 1:1 inclusion complexes (Fig. 5).

Based on the analysis performed, the binding energies of the lupinine and **Lup-T** ligands with the β-cyclodextrin receptor were evaluated. The binding energy was -5.00 kcal/mol for the lupinine complex and -7.17 kcal/mol for the complex with **Lup-T**. In both cases, the negative binding energy values equal to or below -5 kcal/mol indicate effective complex formation between the ligands and **β-CD**. Notably, the more negative binding energy observed for the **Lup-T** complex suggests the formation of a more stable inclusion complex. In the case of the lupinine-**β-CD** complex, the formation of an intermolecular hydrogen bond was identified between the hydroxyl group of lupinine and a secondary oxygen atom of cyclodextrin.

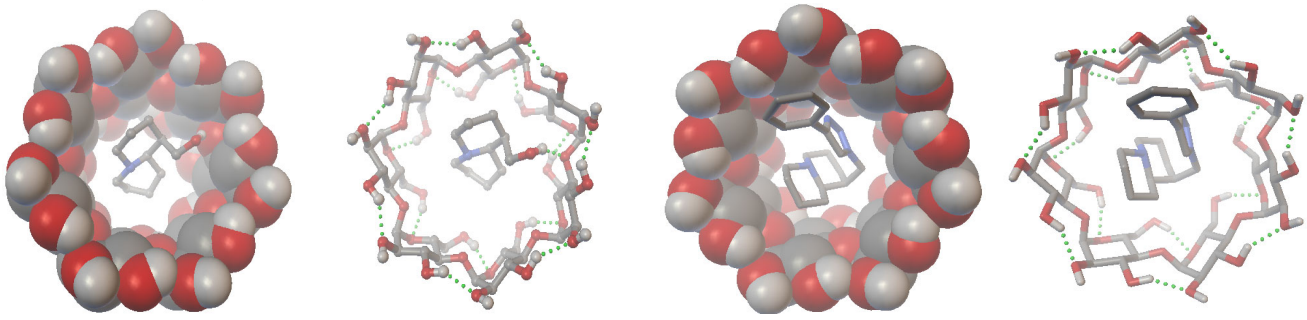

a) 3D model b) Model with 15 h-bonds c) 3D model d) Model with 14 h-bonds

Fig. 5. Docked poses of best-ranked docking score of Lup and Lup-T with b-CD (front view): (a, b) lupinine (binding energy is -5.00 kcal/mol); (c, d) (1S,9aR)-1-[(4-phenyl-1H-1,2,3-triazol-1-yl)methyl]octahydro-1H-quinolizine (binding energy is –7.17 kcal/mol).

2.2.1 Study of the structure of the obtained Lup:β-CD supramolecular inclusion complexes

The structure of the obtained **Lup-T:β-CD** (1:2) inclusion complex was confirmed by FT-IR spectroscopy, ^{1}H and ^{13}C NMR spectroscopy, as well as two-dimensional COSY (^{1}H–^{1}H) and HMQC (^{1}H–^{13}C) spectra. Figure 6a-c presents the FT-IR spectra of lupinine (a), **β-CD** (b), and the **Lup:β-CD** (1:2) clathrate complex (c). In the FT-IR spectrum of lupinine, the O-H stretching vibrations appear as a broad band at 3434 cm^{-1}, while the bending vibrations of the O-H bond are also clearly observed at 1647 and 1614 cm^{-1}. The C-H stretching vibrations of the quinolizidine skeleton are found in the characteristic region of 2928-2757 cm^{-1}, and their bending vibrations appear in the region of 1402-1354 cm^{-1}. The C-O bond vibrations are observed in the range of 1100–1041 cm^{-1}.

The FT-IR spectra of the inclusion compounds revealed changes in the spectral characteristics of the guest molecule; the intensities of the bands at 1450, 1354, 1041, and 873 cm^{-1} nearly disappeared. In the spectra of the **Lup:β-CD** (1:2) clathrate complex, slight shifts in the characteristic absorption bands of the **β-CD** functional groups were observed, indicating the absence of covalent interactions between lupinine and the internal functional groups of **β-CD**. The C-H bond vibrations in CH and CH_2 groups appear with low intensity in the region around 2936 cm^{-1}. The absorption bands at 1641 and 1614 cm^{-1} correspond to the bending vibrations of the O-H bond in COH groups, while the bands at 1415, 1354, 1153, and 1026 cm^{-1} are attributed to bending vibrations of the C-H bonds in the CH_2OH and CHOH groups of the cyclodextrin molecule. In the IR spectra of both **β-CD** and the **Lup:β-CD** complex, the O-H stretching vibrations appear as broad bands with maxima in the range of 3387–3435 cm^{-1} in all binary systems. Thus, the stretching and bending vibrations of the O-H bond and other groups characteristic of the lupinine molecule are not observed in the IR spectra of the **Lup:β-CD** complex. This may indicate that the very broad and intense bands of β-CD masked these groups in the same wavelength range.

The study of host-guest supramolecular inclusion complexes between β-cyclodextrin (**β-CD**) and various substrates by ^{1}H and ^{13}C NMR spectroscopy is based on analyzing the differences in chemical shift (δ) values of the ^{1}H and ^{13}C nuclei in the lupinine substrate and the **β-CD** receptor in their free forms and within the complexes [27-31]. The encapsulation of the substrate (lupinine) is accompanied by non-covalent (hydrophilic) interactions with specific atoms, which lead to shifts in the ^{1}H and ^{13}C NMR signals

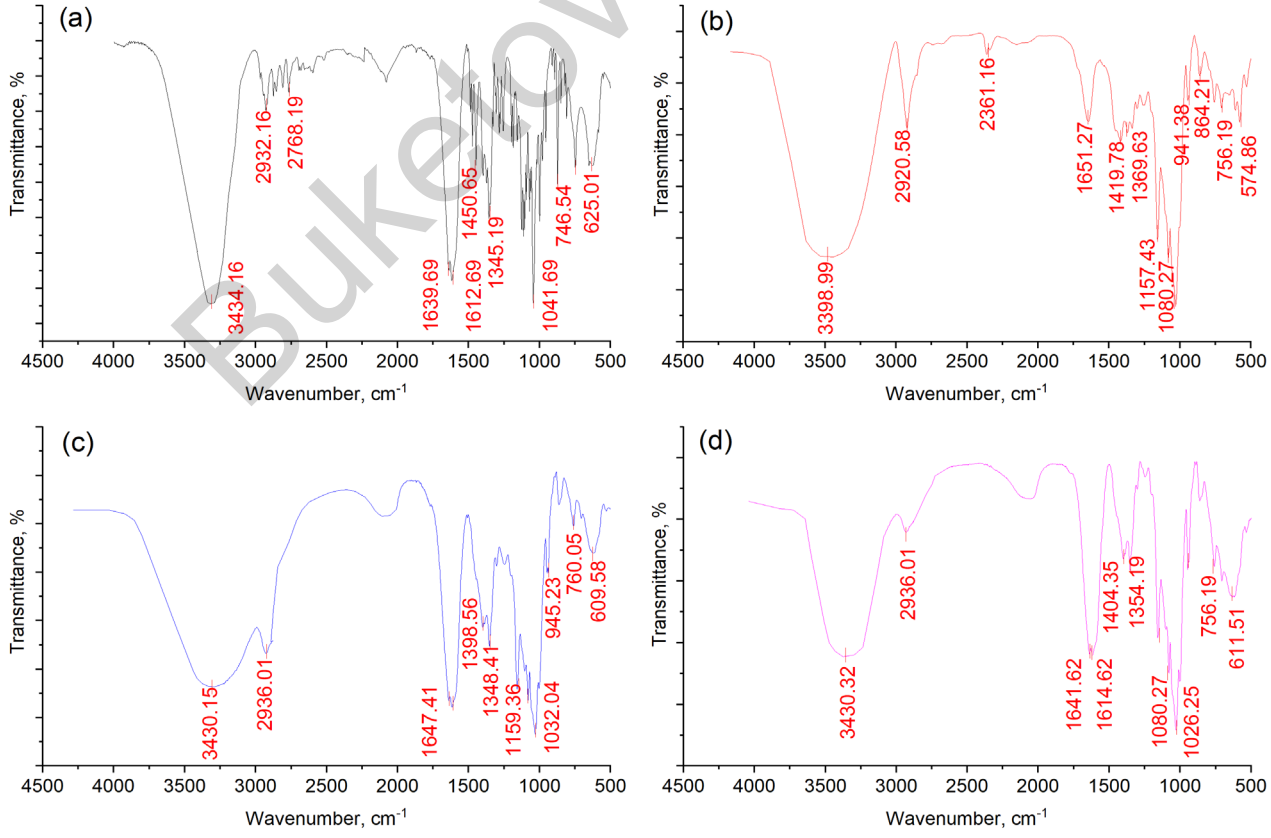

Fig. 6. FT-IR spectra of **Lup** (a), **β-CD** (b), the physical mixture **Lup+β-CD** (c), and the **Lup:β-CD** (1:2) clathrate complex (d).

along the δ scale. Equivalent proton signals from the fused ring system of lupinine appear in the spectrum of the inclusion complex with **β-CD** in the regions of 1.00–1.62 and 1.76–1.92 ppm. The methylene proton signal adjacent to the hydroxyl group is shifted to 3.49–3.50 ppm as a result of complex formation. The secondary carbon atoms of the fused ring system of the lupinine molecule give rise to signals at 21.59, 25.40, 27.35, and 29.33 ppm. The C-6 methine carbon is observed at 25.69 ppm. Downfield signals corresponding to C-2, C-10, C-9, and C-11 also exhibit slight shifts and appear at 57.28, 64.62, and 60.56 ppm. For the carbon atoms of **β-CD**, the chemical shift differences (Δδ) range from 0.03 to 0.25 ppm (Table 1).

For **β-CD** protons, the formation of the inclusion complex is accompanied by downfield shifts of all ^{1}H nuclei. The largest chemical shift differences (Δδ = +0.10-0.12 ppm) are observed for the inner cavity protons H-3 and H-5 of β-cyclodextrin (**β-CD**). In the case of ^{13}C NMR spectra of the substrate, the host, and their complex, more significant signal shifts are observed. Based on the obtained data, the formation of an internal (inclusion) complex with the lupinine molecule can be confirmed (Table 1). The structure of the supramolecular complex is further supported by COSY (^{1}H-^{1}H) spectral data. Analysis of the ^{1}H and ^{13}C NMR spectra indicates the absence of covalent interactions between lupinine and the internal functional groups of the **β-CD** torus. The formation of the clathrate complex is primarily driven by non-specific (dispersive and van der Waals) interactions [32].

2.2.2 Thermal analysis of lupinine and its derivatives by differential thermogravimetry and differential scanning calorimetry

The combined use of various characterization methods, depending on the physical state of the studied samples, provides the most reliable results in terms of model accuracy and consistency [32]. In this regard, it was of interest to compare the energetic and thermodynamic characteristics of lupinine, (1S,9aR)-1-[(4-phenyl-1H-1,2,3-triazol-1-yl)methyl] octahydro-1H-quinolizine (**Lup-T**), and the inclusion complex **Lup-T:β-CD** (1:2). The thermal stability of the samples was evaluated using differential scanning calorimetry (DSC) [33, 34]. The thermogravimetric analysis parameters for the decomposition of the compounds are presented in the TG/DTG curves (Fig. 7a-c). The thermal stability of **Lup**, **Lup-T**, and the **Lup-T:β-CD** (1:2) inclusion complex was investigated under isothermal conditions (Fig. 7).

Table 1. ^{1}H and ^{13}C chemical shifts of lupinine and **β-CD** in the free state and in the inclusion complex

Atom number	Group	δ_0 value in the free state, ppm		δ value in the complex, ppm		Chemical shift change $\Delta\delta(\delta-\delta_0)$, ppm	
	CH_x	δ(^{1}H)	δ(^{13}C)	δ(^{1}H)	δ(^{13}C)	Δδ(^{1}H)	Δδ(^{13}C)
1	2	3	4	5	6	7	8
				lupinine			
1	-CH_2-N	1.90	57.29	1.92	57.28	0.02	-0.01
2	-CH_2-	1.36	21.62	1.34	21.59	-0.02	-0.03
3	-CH_2-	1.34	29.35	1.32	29.33	-0.02	-0.02
4	>CH-	1.58	41.01	1.57	41.03	-0.01	0.02
5	>CH-	1.17	25.58	1.20	25.69	0.03	0.11
6	-CH_2-	1.65	27.40	1.64	27.42	-0.01	0.02
7	-CH_2-	1.37	25.40	1.38	25.40	0.01	0
8	-CH_2-	1.82	64.66	1.83	64.62	0.01	-0.04
9	-CH_2-N	2.66	57.29	2.66	57.28	0	-0.01
10	-CH_2-OH	3.56	60.45	3.55	60.49	-0.01	0.04
				β-cyclodextrin			
1	>CH-	4.77	102.43	4.79	102.68	0.02	0.25
2	>CH-	3.27	72.87	3.30	72.90	0.03	0.03
3	>CH-	3.49	73.54	3.61	73.69	0.12	0.15
4	>CH-	3.30	82.00	3.33	82.15	0.03	0.15
5	>CH-	3.45	72.52	3.55	72.66	0.10	0.14
6	CH_2-	3.57	60.40	3.61	60.56	0.04	0.16

According to the thermogravimetric analysis, the mass loss of the studied compounds occurs differently. Thus, lupinine loses 85% of its mass within the temperature range corresponding to the main heat release. Further mass loss (15%) in the range of 260-300 °C occurs at a low rate and with minimal heat evolution. The most thermally stable compound, **Lup-T**, undergoes single-stage decomposition with a 93% mass loss in the range of 350–400 °C (Fig. 7b).

The thermograms of **Lup-T** (Fig. 7b) and the inclusion complex **Lup-T:β-CD** (1:2) (Fig. 7c) show characteristic thermal peaks at approximately 350 °C, corresponding to the melting points of these compounds. The kinetic parameters of the thermal decomposition of **Lup**, **Lup-T**, and **Lup-T:β-CD** (1:2) were calculated using the model-free Friedman (FR) [35] and Ozawa-Flynn-Wall (OFW) [36] approaches. These methods were selected due to their ability to compare the apparent activation energies of **Lup-T** and the **Lup-T:β-CD** (1:2) clathrate obtained by both differential and integral methods.

Analysis of the obtained data in Arrhenius coordinates allows for the determination of the kinetic parameters of the thermal decomposition reactions $k = A \cdot exp^{-E/RT}$, which are presented in Fig. 8 and Table 2.

Table 2. Activation energy values of **Lup**, **Lup-T**, and **Lup-T:β-CD** (1:2) under various ratios in a nitrogen atmosphere

Sample	$\overline{A}$, s^{-1}	$\overline{E}_{FR}$, kJ·mol^{-1}	$\overline{A}$, s^{-1}	$\overline{E}_{FWO}$, kJ·mol^{-1}
Lup	1.52 10^9	89.12	0.27	110.46
Lup-T	4.72 10^6	91.01	0.14	112.87
Lup-T:β-CD (1:2)	4.43 10^6	88.88	0.15	109.70

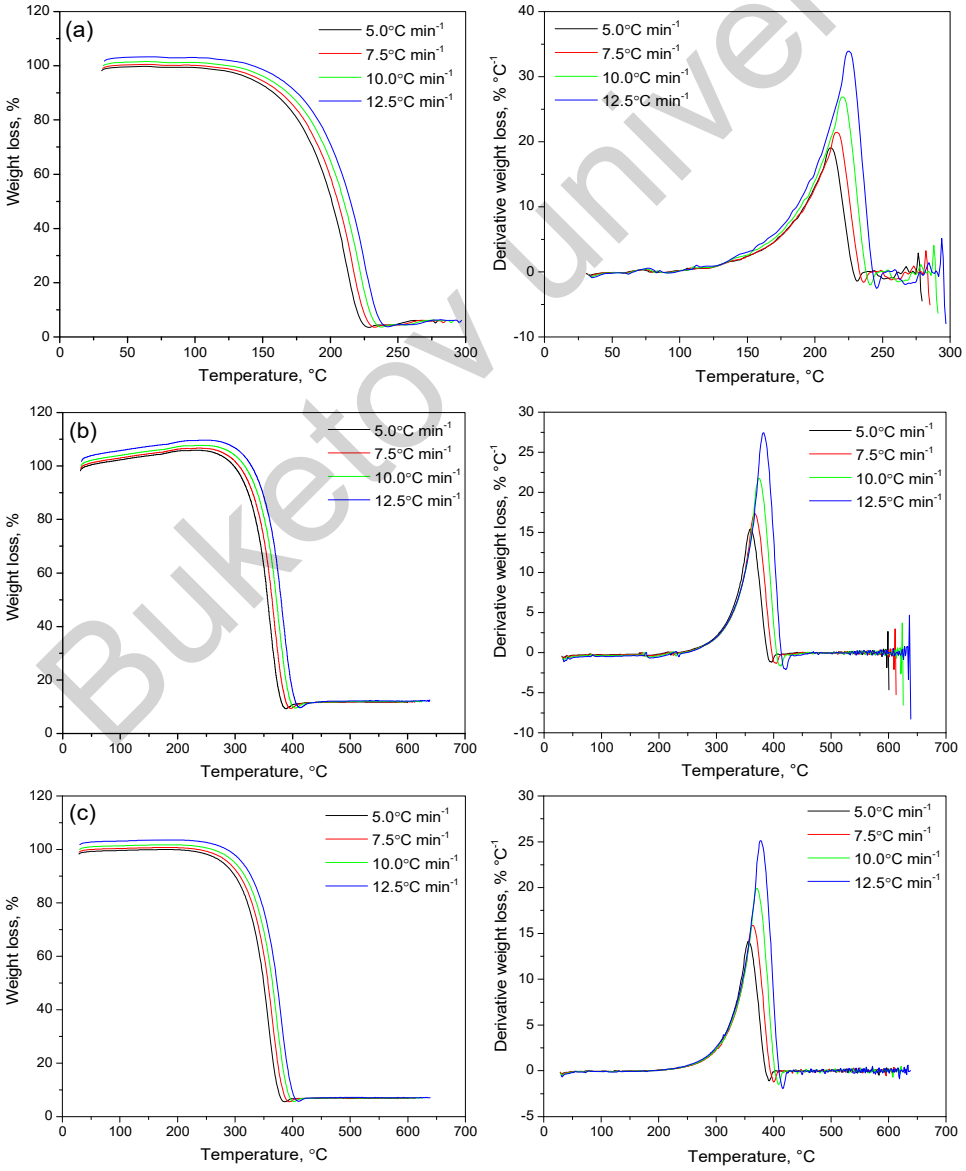

Fig. 7. TG curves of **Lup** (a), **Lup-T** (b), and **Lup-T:β-CD** (1:2) (c).

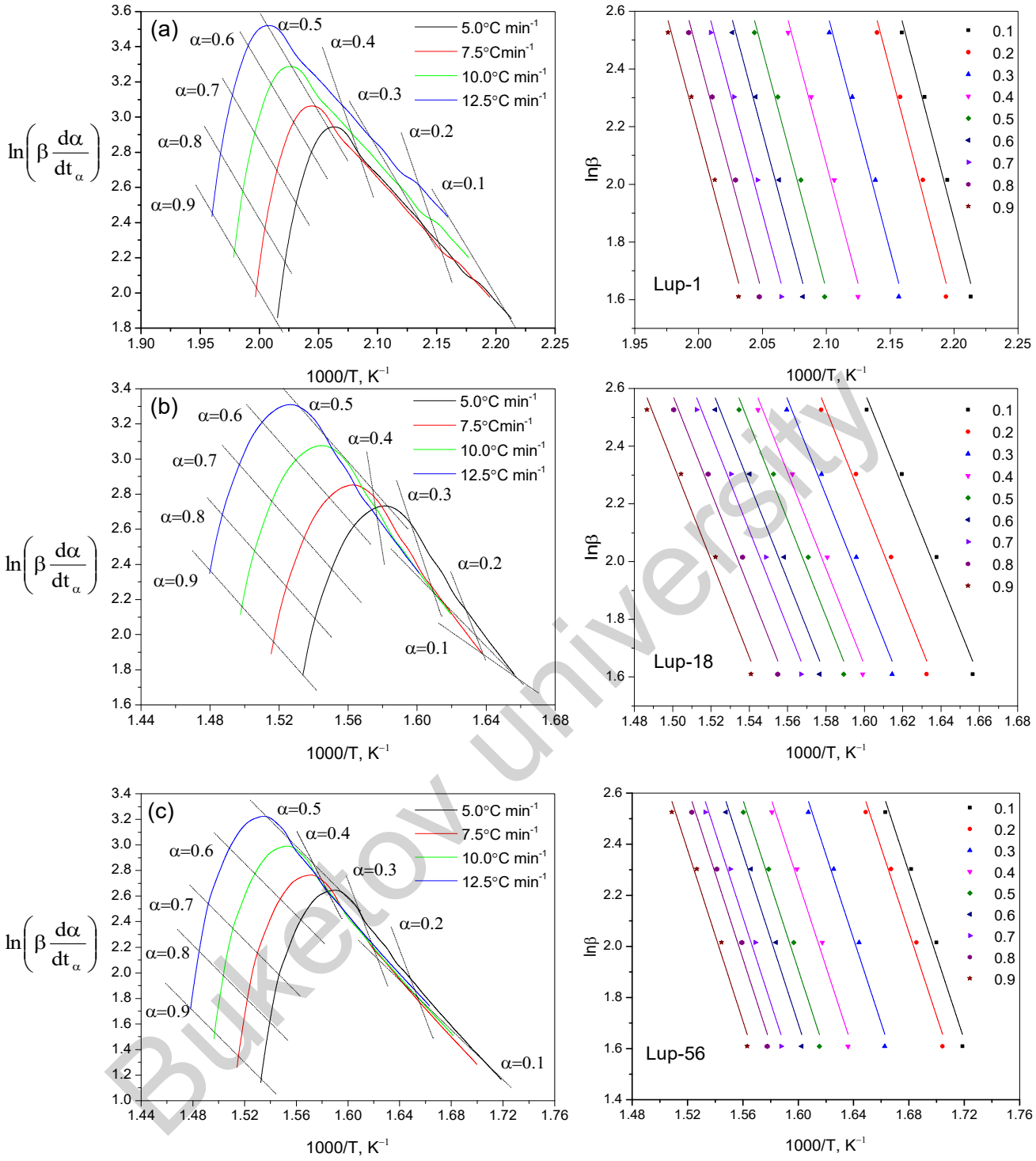

Fig. 8. Graphical analysis results obtained using the Friedman and Ozawa-Flynn-Wall methods for **Lup** (a), **Lup-T** (b), and **Lup-T:β-CD** (1:2) (c) at different heating rates (5-12.5 °C/min).

As shown in Table 2, the kinetic parameters of the thermal decomposition reactions for **Lup**, **Lup-T**, and the inclusion complex **Lup-T:β-CD** (1:2) are of similar magnitude. Figure 9 presents the graphical dependence of the apparent activation energy on the degree of conversion. According to the obtained data, the absence of peaks corresponding to the phase transitions of the individual components in the thermogram of the inclusion complex indicates the formation of a stable **Lup-T:β-CD** (1:2) inclusion complex.

The E–α curves (Fig. 9) obtained using each individual method exhibit similar shapes. As seen from the energy profiles, for α < 0.9, the activation energy (E) values for **Lup-T** are slightly higher than those for the **Lup-T:β-CD** (1:2) complex. As a continuation of

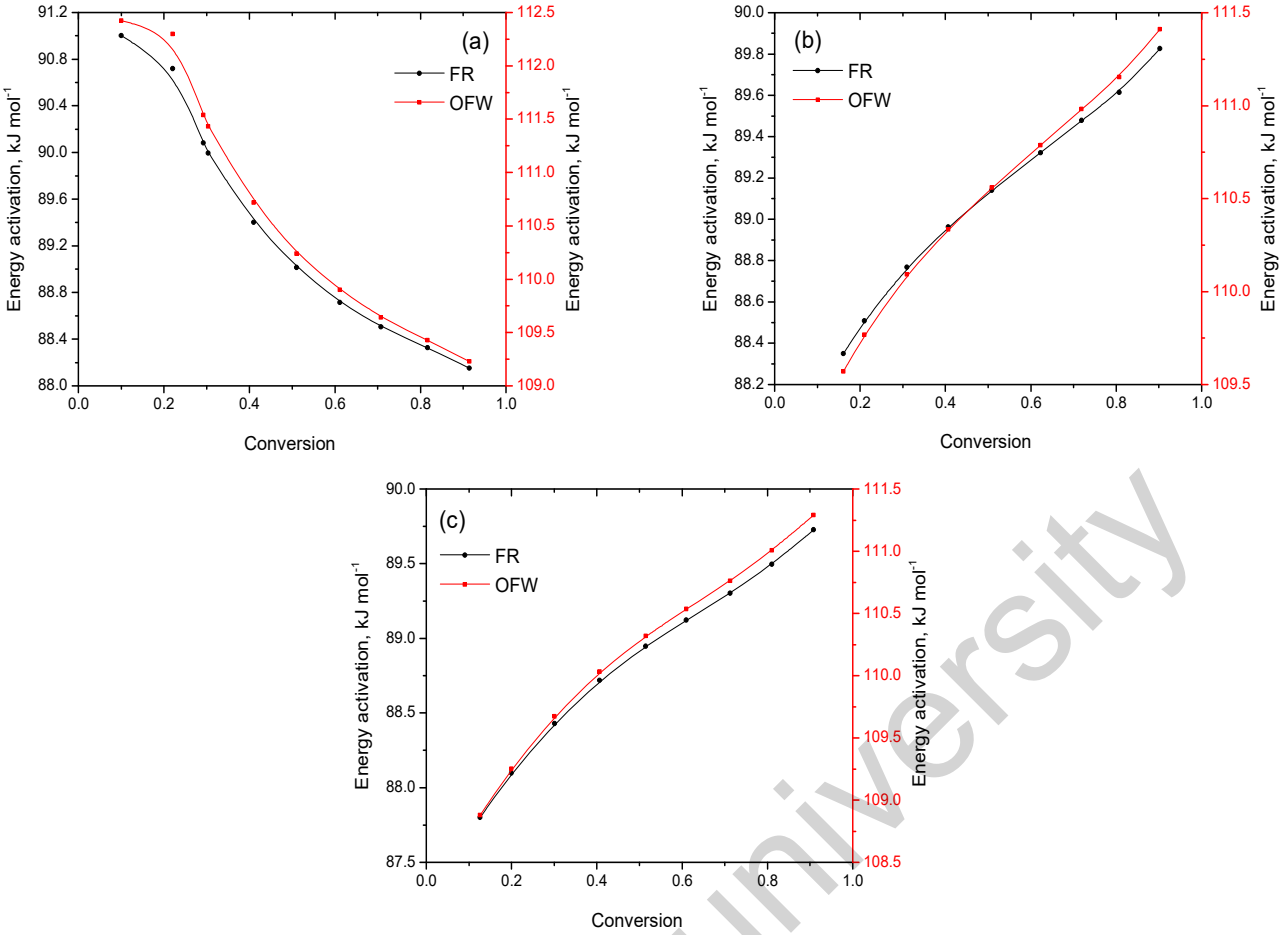

Fig. 9. Profiles of the dependence of apparent activation energy on the degree of conversion according to the Friedman and Ozawa-Flynn-Wall methods for Lup (a), Lup-T (b), and Lup-T:β-CD (1:2) (c).

the study, the non-parametric kinetics method was applied to determine the apparent activation energy. Mathematical processing of the thermogravimetric curves shown in Fig. 12 allows for the calculation of the apparent activation energy using the NPK method, which is based on Eq. (1) [34].

$$r = k(T) \cdot f(\alpha) \quad (1)$$

This method allows for the calculation of all kinetic parameters of a single-step process based on a single differential thermogravimetric curve (Fig. 9). One of the main advantages of this approach is that it does not require specific assumptions regarding the reaction order or the selection of a particular kinetic model function. The authors of studies [36, 37] base their approach on the assumption that, in the NPK method, the reaction rate can be expressed in the form of a matrix

$$M = \{m_{ij}\} = \{k(T_i)f(a_j)\} \quad (2)$$

The most important feature of this method is that the NPK approach employs the singular value decomposition (SVD) algorithm.

$$M = USV^T \quad (3)$$

The elements of matrices U and V are determined by the following expressions

$$f(\alpha) = [u_1, u_2, \ldots u_i] \text{ and } k(T) = [w_1v_1, w_1v_2, \ldots w_1v_i] \quad (4)$$

The reaction rate values obtained at different heating rates were approximated using the non-parametric kinetics method and interpolated as a surface in 3D space ($\beta \cdot d\alpha/dt$, α, T) (Fig. 10). This surface is organized in the form of a matrix $i \times j$, where the rows correspond to different degrees of conversion, from α_1 to α_i, and the columns correspond to temperatures ranging from T_1 to T_j.

One of the equations that effectively describes reactions characterized by a pronounced induction period followed by a sharp increase in reaction rate is the generalized Šesták-Berggren kinetic equation [38].

$$\frac{d\alpha}{dt} = k \cdot \alpha^m (1-\alpha)^n \quad (5)$$

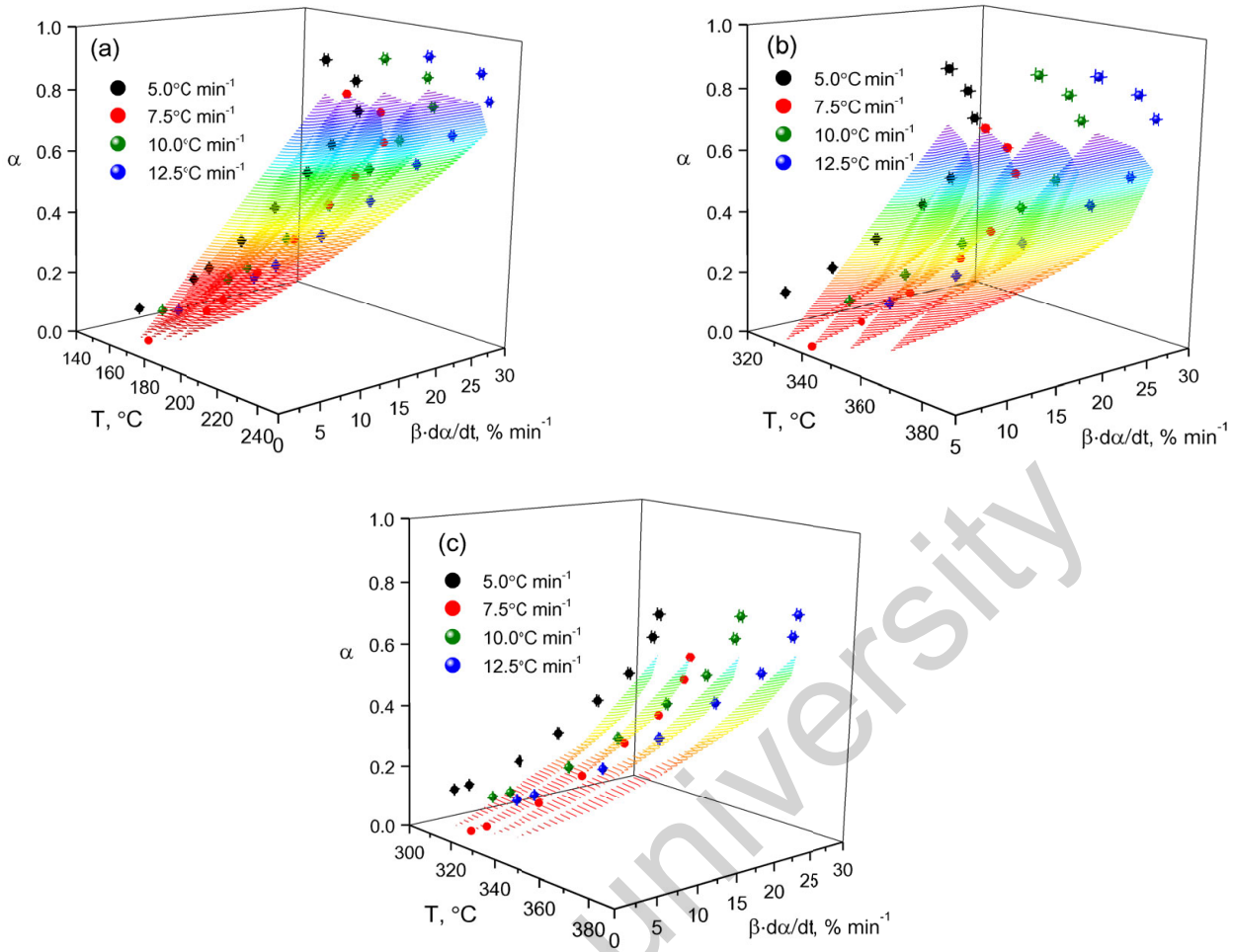

Fig. 10. 3D surface plots for **Lup** (a), **Lup-T** (b), and **Lup-T:β-CD** (1:2) (c) showing the dependence of the reaction rate (β·dα/dt) on temperature (T) and degree of conversion (α) in a nitrogen atmosphere.

The selection of the kinetic function was carried out by fitting the most appropriate model in dα/dt – α coordinates at various heating rates β. The $f(\alpha) = \alpha^m (1 - \alpha)^n$ was used as the $f(\alpha)$ function. The parameters m and n influence the shape and position of the maximum on the dα/dt curve. The results of the kinetic analysis are presented in Fig. 11 and Table 3.

As shown in Fig. 11, the experimental data plotted in dα/dT-α coordinates are well described by the law $f(\alpha) = \alpha^m(1-\alpha)^n$, known as the Šesták-Berggren model [38, 39], under the condition $\frac{dT}{dt}\left(\frac{d\alpha}{dT}\right) = 0$ that $\frac{m}{n} = \frac{\alpha_{max}}{1-\alpha_{max}}$. Table 3 presents the values of the exponents m and n for the experimental data obtained by differential thermal analysis. As seen in Fig. 11c, during the initial stage of decomposition of the **Lup-T** inclusion complex, the reaction rate rapidly increases due to autocatalysis, reaching a maximum at α_{max} = 0.7, followed by a rapid decline until the decomposition nearly ceases completely.

3. Experimental

Molecular modeling of lupinine, (1S,9aR)-1-[(4-phenyl-1H-1,2,3-triazol-1-yl)methyl]octahydro-1H-quinolizine, and β-cyclodextrin (β-CD) was performed using the semi-empirical AM1 method in the Gaussian 2016 software package. The chemical structures were obtained from the PubChem Substance and Compound database (pubchem.ncbi.nlm.nih.gov). Unique chemical structure identifiers are No. 444041 (β-cyclodextrin) and No. 91461 (lupinine). Geometry optimization was carried out in the gas phase (vacuum), without considering solvent effects. Molecular structure files of the receptor and ligands were prepared for docking using ChemBio-Office 2014.

Molecular docking was performed using the Lamarckian Genetic Algorithm (LGA), implemented in AutoDock 4.2.6 and MGLTools 1.5.7. A semi-flexible docking approach was applied, in which the receptor was treated as rigid, while the ligand was allowed

Table 3. Kinetic parameters of the thermal decomposition of **Lup**, **Lup-T**, and **Lup-T:β-CD** (1:2) at various ratios, calculated using the non-parametric kinetics (NPK) method

Sample	$\overline{E}_{NPK}$, kJ·mol^{-1}	$\overline{A}$, s^{-1}	Šesták-Berggren $\alpha^m(1-\alpha)^n$		$\overline{E}_{Sh-B}$	$\overline{A}$, s^{-1}
			m	n		
Lup	89.93	6.49 10^{10}	3.21	1.00	89.13	8.62 10^{10}
Lup-T	90.99	4.71 10^{6}	1.58	0.91	91.00	4.54 10^{7}
Lup-T:β-CD (1:2)	88.83	4.40 10^{6}	2.07	1.00	88.51	9.48 10^{7}

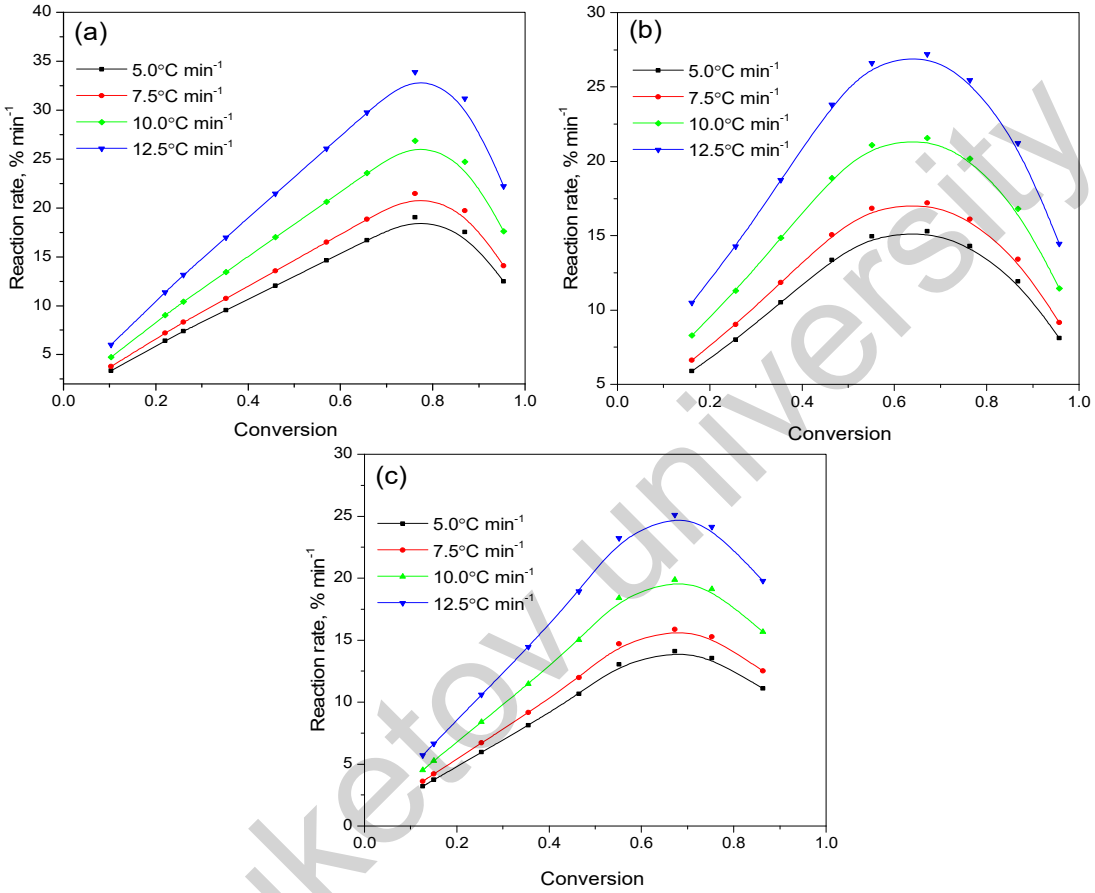

Fig. 11. Approximation of experimental data using f(α) functions based on the Šesták–Berggren method for **Lup** (a), **Lup-T** (b), and **Lup-T:β-CD** (1:2) (c).

to rotate and translate within a predefined cubic grid. AutoDock calculates binding energy using an empirical scoring function based on the free energy of binding, incorporating electrostatic, hydrophobic, and solvation effects, as well as configurational entropy. The AutoDock approach employs Monte Carlo simulated annealing with rapid energy evaluation using grid-based molecular affinity potentials.

Inclusion complexes of lupinine (**Lup:β-CD**) and its derivative (**Lup-T:β-CD**) were obtained by co-precipitation from aqueous-ethanolic solutions of lupinine (and/or its derivative) with β-cyclodextrin (**β-CD**). Stoichiometric amounts of lupinine and **β-CD** (in 1:1, 1:2, and 1:3 molar ratios) were dissolved in a minimal volume of a 1:1 water:ethanol mixture. The solutions were stirred on a magnetic stirrer at 50 °C for 5 hours. The resulting precipitate was filtered, washed with acetone, and dried at 50–52 °C. The inclusion complexes **Lup:β-CD** (1:2; 72.5%) and **Lup-T:β-CD** (1:2; 65.4%) were obtained as white crystalline solids, melting with decomposition at 265–290 °C and 250–280 °C, respectively.

IR spectra of the compounds and their inclusion complexes were recorded using a Cary 600 Series FT-IR spectrometer (Agilent Technologies, USA) in the range of 4000–400 cm^{-1}. The IR samples were prepared as pellets composed of the test substances and KBr.

^{1}H and ^{13}C NMR spectra were recorded on Bruker AV-400 (400 and 101 MHz, respectively) and Bruker DRX-500 (500 and 125 MHz, respectively) spectrometers. The spectra of the compounds were acquired in $CDCl_3$ (Sigma-Aldrich), using the solvent signal (δ_C = 76.9 ppm) and the residual $CHCl_3$ signal (δ_H = 7.24 ppm) as internal standards.

Differential Thermogravimetry (DTG) and Differential Scanning Calorimetry (DSC). Thermal analysis of β-cyclodextrin samples and their inclusion complexes with lupinine and its derivative (sample mass: 12 mg) was performed using differential thermogravimetry (DTG) and differential scanning calorimetry (DSC) on a DTA/DSC thermal analyzer (Setaram). All calculations were carried out using Mathcad software.

4. Conclusions

Encapsulated clathrate complexes of including the alkaloid lupinine and its 1,2,3-triazole derivative using the oligosaccharide β-cyclodextrin were obtained. Obtaining supramolecular complexes of lupinine inclusion and its new triazole derivative will make it possible to create a new water-soluble dosage form in the future. Using molecular modeling methods and optimization of the geometry of the molecules of the objects of study made it possible to establish that the size of the internal hydrophobic cavity of the β-cyclodextrin molecule is sufficient for the formation of inclusion complexes with lupinine and its triazole derivatives.

Acknowledgments

The work was financially supported by the Committee of Science of the Ministry of Science and Higher Education of the Republic of Kazakhstan (grant number AP23487712).

References

[1]. J.P. Michael, Indolizidine and quinolizidine alkaloids, *Nat. Prod. Rep.* 19 (2002) 719–741. DOI: 10.1039/b104969k

[2]. J.P. Michael, Simple indolizidine and quinolizidine alkaloids: in The Alkaloids: Chemistry and Biology, Academic Press, 2001, pp. 91–258. DOI: 10.1016/S0099-9598(01)55004-X

[3]. K.I. Takao, R. Munakata, K.I. Tadano, Recent Advances in Natural Product Synthesis by Using Intramolecular Diels–Alder Reactions, *Chem. Rev.* 105 (2005) 4779–4807. DOI: 10.1021/cr040632u

[4]. S.C.Q. Magalhães, F. Fernandes, A.R.J. Cabrita, et al., Alkaloids in the valorization of European *Lupinus* spp. seeds crop, *Ind. Crops Prod.* 95 (2017) 286–295. DOI: 10.1016/j.indcrop.2016.10.033

[5]. E.L. Konrath, C. Dos Santos Passos, L.C. Klein-Junior, A.T. Henriques, Alkaloids as a source of potential anticholinesterase inhibitors for the treatment of Alzheimer's disease, *J. Pharm. Pharmacol*. 65 (2013) 1701–1725. DOI: 10.1111/jphp.12090

[6]. R.T. Tlegenov, D.N. Dalimov, Kh.Kh. Khaitbaev, et al., Synthesis and anticholinesterase activites of a number of derivatives of the alkaloid lupinine, *Chem. Nat. Compd.* 26 (1990) 434–436. DOI: 10.1007/BF00598999

[7]. Z.S. Nurmaganbetov, O.A. Nurkenov, A.I. Khlebnikov, et al., Antiviral Activity of (1S,9aR)-1-[(1,2,3-Triazol-1-yl)methyl]octahydro-1H-quinolizines from the Alkaloid Lupinine, *Molecules* 29 (2024) 5742. DOI: 10.3390/molecules29235742

[8]. K.M. Frik, L.G. Kamphuis, K.M. Siddique, et al., *Front. Plant Sci.* 31 (2017) 87. DOI: 10.3389/fpls.2017.00087

[9]. N.K. Gusarova, S.F. Malysheva, L.A. Oparina, et al., Synthesis of novel alkaloid derivatives from vinyl ether of lupinine and PH-addends, *Arkivoc* 7 (2009) 260–267. DOI: 10.3998/ark.5550190.0010.725

[10]. A.A. Abduvakhabov, R. Tlegenov, K.K. Khaitbaev, et al., Synthesis of lupinine esters and their interaction with cholinesterases, *Chem. Nat. Compd.* 26 (1990) 60–63. DOI: 10.1007/BF00605202

[11]. D. Su, X. Wang, C. Shao, et al., Total Synthesis of (+)-Epilupinine via An Intramolecular Nitrile Oxide-Alkene Cycloadditio, *J. Org. Chem.* 76 (2011) 188–194. DOI: 10.1021/jo101910r

[12]. V.E. Semenov, I.V. Zueva, M.A. Mukhamedyarov, et al., 6-Methyluracil Derivatives as Bifunctional Acetylcholinesterase Inhibitors for the Treatment of Alzheimer's Disease, *Chem. Med. Chem.* 11 (2015) 1863–1874. DOI: 10.1002/cmdc.201500334

[13]. M. Ahari, A. Perez, C. Menant, et al., A Direct Stereoselective Approach to trans-2,3-Disubstituted Piperidines: Application in the Synthesis of 2-Epi-CP-99,994 and (+)-Epilupinine, *Org. Lett.* 10 (2008) 2473–2476. DOI: 10.1021/ol800722a

[14]. A. Boido, I. Vazzana, F. Sparatore, et al., Preparation and pharmacological activity of some 1-lupinylbenzimidazoles and 1-lupinylbenzotriazoles, *Farmaco* 46 (1991) 775–788. PMID: 1772563.

[15]. A. Sparatore, N. Basilico, S. Parapini, et al., 4-Aminoquinoline quinolizidinyl- and quinolizidinylalkyl-derivatives with antimalarial activity, *Bioorg. Med. Chem*. 13 (2005) 5338–5345. DOI: 10.1016/j.bmc.2005.06.047

[16]. B. Tasso, F. Novelli, M. Tonelli, et al., Synthesis and Antiplasmodial Activity of Novel Chloroquine Analogues with Bulky Basic Side Chains, *Chem. Med. Chem.* 10 (2015) 1570–1583. DOI: 10.1002/cmdc.201500195

[17]. N. Erdemoglu, S. Ozkan, F. Tosun, Alkaloid profile and antimicrobial activity of Lupinus angustifolius L. alkaloid extract, *Phytochem. Rev*. 6 (2007) 197–201. DOI: 10.1007/s11101-006-9055-8

[18]. J.K. Przybylak, D. Ciesiołka, W. Wysocka, et al., Alkaloid profiles of Mexican wild lupin and an effect of alkaloid preparation from Lupinus exaltatus seeds on growth and yield of paprika (Capsicum annuum L.), *Ind. Crops Prod.* 21 (2005) 1–7. DOI: 10.1016/j.indcrop.2003.12.001

[19]. I.A. Schepetkin, Z.S. Nurmaganbetov, S.D. Fazylov, et al., Inhibition of Acetylcholinesterase by Novel Lupinine Derivatives, *Molecules* 28 (2023) 3357. DOI: 10.3390/molecules28083357

[20]. C. Russoni, N. Vaiana, M. Casagranda, et al., Synthesis and comparison of antiplasmodial activity of (+), (−) and racemic 7-chloro-4-(N-lupinyl)aminoquinoline, *Bioorg. Med. Chem*. 20 (2012) 5980–5985. DOI: 10.1016/j.bmc.2012.07.041

[21]. D.V. Katorov, G.F. Rudakov, I.N. Katorova, et al., Synthesis of 1,2,3-triazoles from heterocyclic α-nitro azides, *Russ. Chem. Bull.* 61 (2012) 2114–2123. DOI: 10.1007/s11172-012-0296-y

[22]. N. Adki, N. Rana, R. Palthya, Synthesis and biological evaluation of pyrazol analogues linked with 1,2,3-triazol and 4-thiazolidinone as antimicrobial agents, *Curr. Chem. Lett.* 11 (2022) 139–146. DOI: 10.5267/j.ccl.2021.001

[23]. M. Srinivas, A.S. Pathania, P. Mahajan, et al., Design and synthesis of 1,4-substituted 1H-1,2,3-triazolo-quinazolin-4(3H)-ones by Huisgen 1,3-dipolar cycloaddition with PI3Kγ isoform selective activity, *Bioorg. Med. Chem. Lett*. 28 (2018) 1005–1010. DOI: 10.1016/j.bmcl.2018.02.032

[24]. A.O. Finke, M.E. Mironov, A.B. Skorova, E.E. Shults, Copper-catalyzed 1,3-dipolar cycloaddition reaction of spirosolanederived azide for the preparation of modified solasodine alkaloid, *Chem. Heterocycl. Compd.* 54 (2018) 411–416. DOI: 10.1007/s10593-018-2284-0

[25]. A. Sahu, Advance Synthetic Approaches to 1,2,3-triazole Derived Compounds: State of the Art 2004-2020, *Curr. Organocatal.* 8 (2021) 271–288. DOI: 10.2174/2213337208666210428123033

[26]. O.A. Nurkenov, Z.S. Nurmaganbetov, S.D. Fazylov, et al., Synthesis, structure and biological activity of (1S,9aR)-1H-1,2,3-triazol-1-yl)methyl)octahydro-1H-quinolizine derivatives of lupinine, *Arch. Razi Inst.* 77 (2022) 2307–2317. https://archrazi.areeo.ac.ir/article_127604.html

[27]. C.W. Tornoe, C. Christensen, M. Meldal, Peptidotriazoles on Solid Phase: [1,2,3]-Triazoles by Regiospecific Copper(I)-Catalyzed 1,3-Dipolar Cycloadditions of Terminal Alkynes to Azides, *J. Org. Chem.* 67 (2002) 3057–3064. DOI: 10.1021/jo011148j

[28]. P. Wu, V.V. Fokin, Catalytic Azide–Alkyne Cycloaddition: Reactivity and Applications, *Aldrichimica Acta* 40 (2007) 7–17. DOI: 10.1002/chin.200736242

[29]. X. Creary, A. Anderson, C. Brophy, et al., Method for Assigning Structure of 1,2,3-Triazoles, *J. Org. Chem.* 77 (2012) 8756–8761. DOI: 10.1021/jo301265t

[30]. S.K. Upadhyay, G. Kumar, NMR and molecular modelling studies on the interaction of fluconazole with β-cyclodextrin, *Chem. Cent. J.* 3 (2009) 1–9. DOI: 10.1186/1752-153X-3-9

[31]. S.V. Kurkov, T. Loftsson, Cyclodextrins, *Int. J. Pharm.* 453 (2013) 167–180. DOI: 10.1016/j.ijpharm.2012.06.055

[32]. M. Burkeev, S. Fazylov, R. Bakirova, et al., Thermal decomposition of β-cyclodextrin and its inclusion complex with vitamin E, *Mendeleev Commun*. 31 (2021) 76–78. DOI: 10.1016/j.mencom.2021.01.023

[33]. R. Serra, J. Sempere, R. Nomen, A new method for the kinetic study of thermoanalytical data: The non-parametric kinetics method, *Thermochim. Acta* 316 (1998) 37–45. DOI: 10.1016/S0040-6031(98)00295-0

[34]. H.L. Friedman, Kinetics of thermal degradation of char-forming plastics from thermogravimetry. Application to a phenolic plastic, *J. Polym. Sci.* 6 (1964) 183–195. DOI: 10.1002/polc.5070060121

[35]. J.H. Flynn, L.A. Wall, A quick, direct method for the determination of activation energy from thermogravimetric data, *Polym. Lett.* 4 (1966) 323–328. DOI: 10.1002/pol.1966.110040504

[36]. R. Serra, R. Nomen, J. Sempere, The Non-Parametric Kinetics A New Method for the Kinetic Study of Thermoanalytical Data, *J. Therm. Anal. Calorim.* 52 (1998) 933–943. DOI: 10.1023/A:1010120203389

[37]. M.E. Wall, A. Rechtsteiner, L.M. Rocha, Singular Value Decomposition and Principal Component Analysis, *A Pract. Approach Microarray Data Anal.* 9 (2002) 91–109. DOI: 10.1007/0-306-47815-3_5

[38]. J. Šesták, G. Berggren, Study of the kinetics of the mechanism of solid-state reactions at increasing temperatures, *Thermochim. Acta* 3 (1971) 1–12. DOI: 10.1016/0040-6031(71)85051-7

[39]. X. Zhang, Applications of Kinetic Methods in Thermal Analysis: A Review, *Engineered Science* 14 (2021) 1–13. DOI: 10.30919/es8d1132